

FINITE DIFFERENCE TIME-DOMAIN METHOD FOR SIMULATING DIELECTRIC MATERIALS AND METAMATERIALS

A. HENDI^a, F. ALKALLAS^a, H. ALMOUSSA^b, H. ALSHAHRI^b,
M. ALMONEEF^a, M. ALENAZY^a, N. ALSAIF^a, A. ALTOWYAN^a,
A. LAREF^b, M. AWAD^b, K. ORTACHI^b

^a*Department of Physics, College of Science, Princesses Nourah Bint Abdulrahman University, Riyadh, Saudi Arabia*

^b*Department of Physics, College of Science, King Saud University, Saudi Arabia*

In this study, Finite Difference Time Domain (FDTD) is employed to model and simulate both dielectric materials and metamaterials. Interestingly, the metamaterials own very peculiar characteristics that are related to the simultaneous negative permittivity and permeability. Based on FDTD technique, we can simulate the electromagnetic devices with the inclusion of the simultaneous electric and magnetic fields over time. The striking features of metamaterials illustrate the increase and backward propagation as well as the energy absorption in one-dimensional (1D) or two-dimensional (2D) systems. These systems could have potential applications, such as metamaterial superlens.

(Received February 19, 2020, Accepted July 24, 2020)

Keywords: FDTD, Negative permittivity, Metamaterials, Superlens

1. Introduction

During the past few years, a new technique for designing electromagnetic structures has been suggested, where the electromagnetic waves could be modulated within a material by incorporating the spatial variation in the constitutive parameters. The triggered notion of metamaterials aroused a great deal of consideration of scientists for this kind of stimulating applications in various frequency regimes from microwave, terahertz (THz), infrared (IR), optics, and acoustics, etc. In aerospace functionalities, invisibility yields prohibiting information about an object to attain radar-like detectors [1-6].

The Finite Difference Time Domain (FDTD) method, represents a powerful and an effective technique that is extensively employed with successful manner for simulating and modeling the electromagnetic wave interaction at different frequencies dispersion and non-dispersed materials. In order to establish a new behavior, a manipulation through the dielectric and magnetic response of a material is necessary. At this stage, it is feasible to involve metamaterials as an effective medium tailored to acquire the desirable macroscopic characteristics via sub-wavelength design. The prosperous fabrication of such metamaterials, emerged a prominent consideration in the exploration of metamaterials by scientists from the diverse arenas. The realization of metamaterials paved the pathway for various tremendous applications, such as sub-wavelength imaging, solar cell design, and antennas [7-13].

The purpose of this work is to simulate the propagating electromagnetic waves both in dielectric material and metamaterial (1D and 2D systems) by employing FDTD technique, while the description of the method as well as the softwares that were used and changed according to our simulated results, are provided in Refs. [13,14]. Also, we are mainly concerned by involving the effect of varying the lattice cells in x-y directions, waveguides and dielectric constants of the medium on the variation of propagating electromagnetic wave in 1D and 2D-systems.

2. Method of simulation: Finite Difference Time-Domain method

The FDTD is one of a commonly used technique for the solution of electromagnetic problems. Both conceptually and in terms of implementation, it can accurately tackle a wide range of problems even for programming three-dimensional systems. The FDTD method employs finite differences as approximations to both the spatial and temporal derivatives that appear in Maxwell's equations (specifically Ampere's and Faraday's laws) [14].

2.1. FDTD in two dimensions

We will start with the Maxwell's normalized equations [14]:

$$\frac{\partial D}{\partial t} = \frac{1}{\sqrt{\epsilon_0 \mu_0}} \nabla \times H \quad (1)$$

$$D(\omega) = \epsilon_r(\omega) \cdot E(\omega) \quad (2)$$

$$\frac{\partial H}{\partial t} = -\frac{1}{\sqrt{\epsilon_0 \mu_0}} \nabla \times E \quad (3)$$

Here D is the electric flux density, H is magnetic field, E is the electric field, ϵ_0 and μ_0 are the permittivity and permeability in vacuum, and ϵ_r is the relative permittivity. In a two-dimensional simulation we need to choose between two modes: (1) the transverse magnetic (TM) mode, which is composed of E_z , H_x , and H_y , or (2) transverse electric (TE) mode, which is composed of E_x , E_y , and H_z . By using the TM modes, the equations above will be reduced to:

$$\frac{\partial D_z}{\partial t} = \frac{1}{\sqrt{\epsilon_0 \mu_0}} \left(\frac{\partial H_y}{\partial x} - \frac{\partial H_x}{\partial y} \right) \quad (4)$$

$$D_z(\omega) = \epsilon_r(\omega) \cdot E_z(\omega) \quad (5)$$

$$\frac{\partial H_x}{\partial t} = -\frac{1}{\sqrt{\epsilon_0 \mu_0}} \frac{\partial E_z}{\partial y} \quad (6)$$

$$\frac{\partial H_y}{\partial t} = \frac{1}{\sqrt{\epsilon_0 \mu_0}} \frac{\partial E_z}{\partial x} \quad (7)$$

To solve an electromagnetic problem, the idea is to simply discretize both in time and space Maxwell's equations with central difference approximations (see figure 1). In this cell electric and magnetic components are distributed half time step shift and half spatial step shift in a way that makes every single electric point surrounded by four magnetic points and vice versa [14].

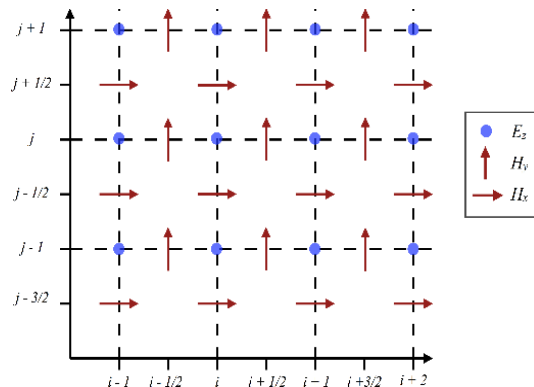


Fig. 1. Interleaving for the two-dimensional TM formulation [14].

By plugging equations (4), (6), and (7) into the finite difference scheme results in:

$$\frac{D_z^{n+1/2}(i,j) - D_z^{n-1/2}(i,j)}{\Delta t} = \frac{1}{\sqrt{\epsilon_0 \mu_0}} \frac{H_y^n(i+1/2,j) - H_y^n(i-1/2,j)}{\Delta x} - \frac{1}{\sqrt{\epsilon_0 \mu_0}} \frac{H_x^n(i,j+1/2) - H_x^n(i,j-1/2)}{\Delta x} \quad (8)$$

$$\frac{H_x^{n+1}(i,j+1/2) - H_x^n(i,j+1/2)}{\Delta t} = -\frac{1}{\sqrt{\epsilon_0 \mu_0}} \frac{E_z^{n+1/2}(i,j+1) - E_z^{n+1/2}(i,j)}{\Delta x} \quad (9)$$

$$\frac{H_y^{n+1}(i+1/2,j) - H_y^n(i+1/2,j)}{\Delta t} = \frac{1}{\sqrt{\epsilon_0 \mu_0}} \frac{E_z^{n+1/2}(i+1,j) - E_z^{n+1/2}(i,j)}{\Delta x} \quad (10)$$

Equation (8) gives the temporal derivative of the electric flux density in term of the spatial derivative of the magnetic field. Conversely, equations (9)-(10) provide the temporal derivative of the magnetic field in terms of the spatial derivative of the electric field [2]. These two equations represent a plane wave traveling in the z-direction [3]. Then it is possible to solve the resulting difference equations to obtain "update equations that express the (unknown) future fields in terms of (known) past fields. The magnetic fields are estimated one time-step into the future so they are now known (effectively they become past fields), while the electric fields one time-step into the future so they are now recognized (actually they become past fields). This procedure can repeat the previous two steps until the fields have been obtained over the desired duration.

Where n is time $t = 4t \cdot n$, the term $n + 1$ means one time step later, and the time step $4t$ is defined by:

$$\Delta t = \frac{\Delta x}{2c} \quad (11)$$

Where c is the speed of light, and $4x$ is the cell size [14].

There are two cases for the determination of electromagnetic (EM) sources, such as the generation of a continuous wave (CW) signal or a short pulse. Always there is a minimum wavelength (maximum frequency) of interest. The cell size must be much smaller than minimum wavelength.

There are typically two general classes of electromagnetic wave sources; the soft source which consists of impressing a current and the hard source which consists of impressing an electric field. The physical meaning of the soft source is well understood and its analytical solution is known [14]. The source may be insert at any node (may be any value between first and last node) by a time dependent source function $g(t)$ (the soft source: Gaussian pulse) as [14]:

$$g(t) = \exp\left\{-\left(\frac{t - t_0}{T}\right)^2\right\} \quad (12)$$

t is the time delay and t_0 indicates pulse width.

We employ in this simulation Gaussian source as source, as describe in Ref [14]. A perfectly matched layer (PML) is commonly used to truncate the computational regions in numerical methods to simulate problems with open boundaries, especially in the FDTD. A PML is an artificial absorbing layer for wave equations, there are several equivalent formulations of PML. ABCs creates a numerical representation that makes a grid with a finite number of electric and magnetic field points to behave as if they were infinite. With these conditions, the wave will be completely “absorbed” by the termination. If a wave is moving to a boundary in free space, it is traveling by speed of light c_0 in one time step in FDTD. The reason for using PML is its effectiveness and versatility in working with different media [14-19]. Here the FDTD technique and the softwares that were modified according to our simulated results, are represented in Refs. [13,14].

3. Results and discussion

3.1. The electric field (E_x and E_y) and magnetic field (H_z) in 2D system

The electric field (E_x and E_y) and magnetic field (H_z) distributions in two dimensional free space and dispersive materials, are simulated by altering the constant dielectric constant and number of cell lattices. A Gaussian pulse was employed with frequencies excitations arising at left side of the x-y cells, which are propagating outward and are absorbed without showing any reflection back in the problem space. The fields at the edge must be propagating outward. The point at the end of the grid reflects any field that is facing it. Reflecting fields make distortion in the problem space. ABCs are necessary to prevent E and H fields reflected back into the problem space.

As displayed in Figs. (2-4), a comparative study was set by varying the dielectric constant of the medium from the free space to dispersive medium. In the beginning, the systems were excited and the electromagnetic waves were propagated along E_x , E_y , and H_z , respectively in circular shape when the time step was varied. The variation of propagating wave depends not only on the variation of medium by changing the dielectric constant, also it depends on the change of the unit cells along x-y directions.

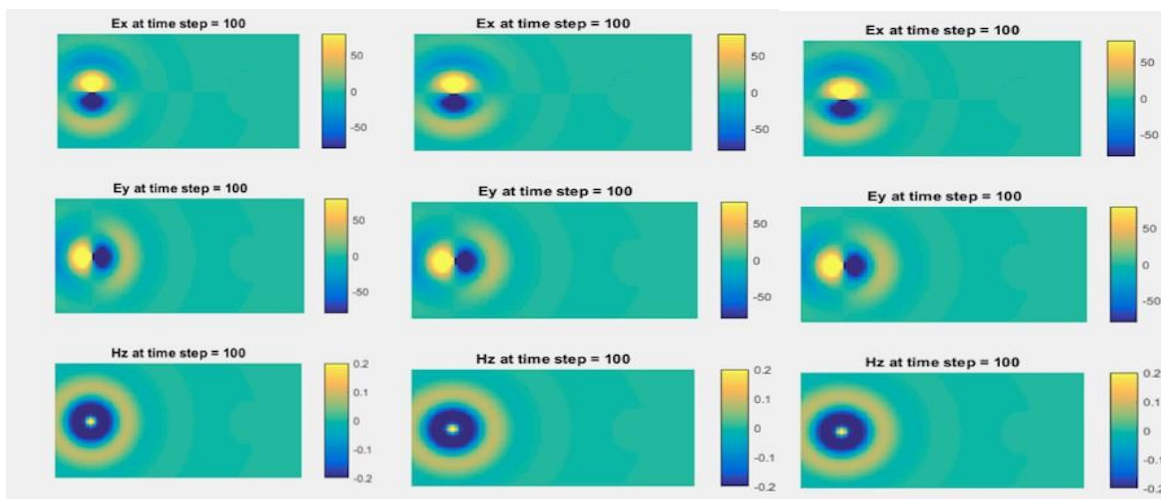


Fig. 2. Electric field propagation at different size cells (4, 8, and 12) and frequency= 5GHz with $\epsilon = 1$ (free space).

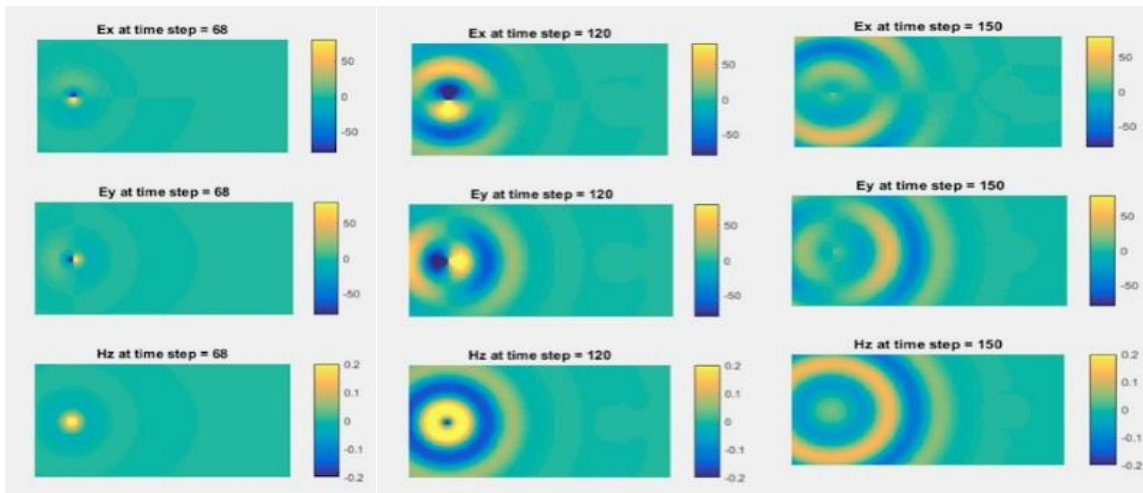


Fig. 3. Electric field propagation at different thickness of layers ($\epsilon=4$) and frequency=5.GHz, unit cell=8 at different time steps.

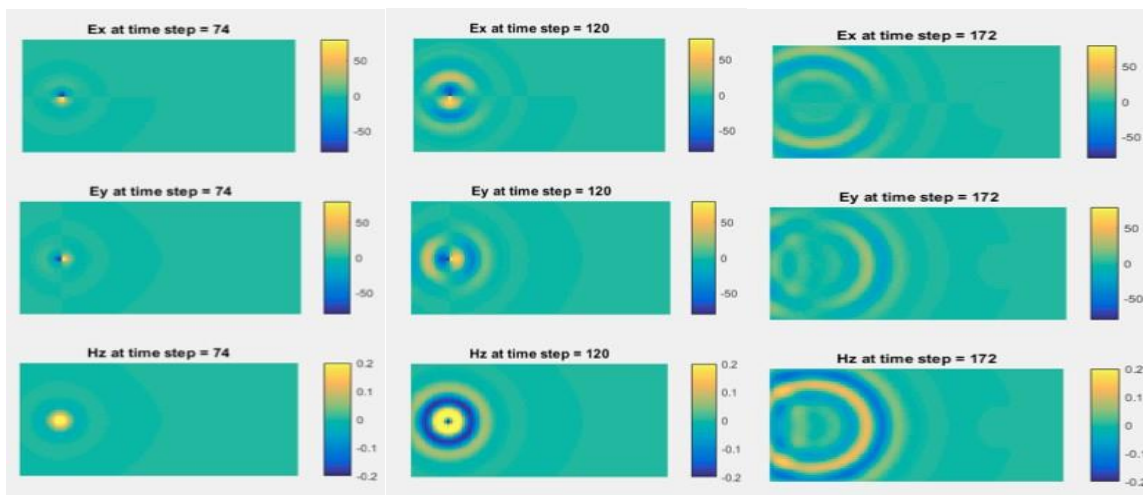


Fig. 4. Electric field propagation at different thickness of layers ($\epsilon=8$) and frequency= 5.0×10^9 Hz, unit cell=8 at different time steps.

3.2. The electric field (E_z) in two dimensional free space and dispersive materials in 2D

The electric field (E_z) in two dimensional free space and dispersive materials are discussed with the alteration of the permittivity value (ϵ) from free space to dispersive medium and the number of cells is varying in plane. To prohibit the reflections from lossy regions, the boundaries of absorbing grid is necessary for outgoing waves, by using perfectly matched layers. A Gaussian pulse was started in the center of cell along x-y directions by using PML. The cell size and number of step are varied to see their effect on the change of the propagating wave. The simulated results of the electric field along z-axis are displayed in figures (5-7) by changing the size cells along x-y directions and by varying the dielectric constant from free space to dielectric materials. The propagation of the wave nature at the central point is varied according to the variation of the thickness and medium when the time step is modified from the starting of the wave excitation until the absorption of the wave at the central region, which are determined at various dielectric constants. It is well noticed that the electric field at early time response is approximately the same at all different dielectric constants when the number of layers is equal to 100. However, the propagating wave is varying at the end of time step and this is due to the fact that the medium is more dispersive when the dielectric constant is increased.

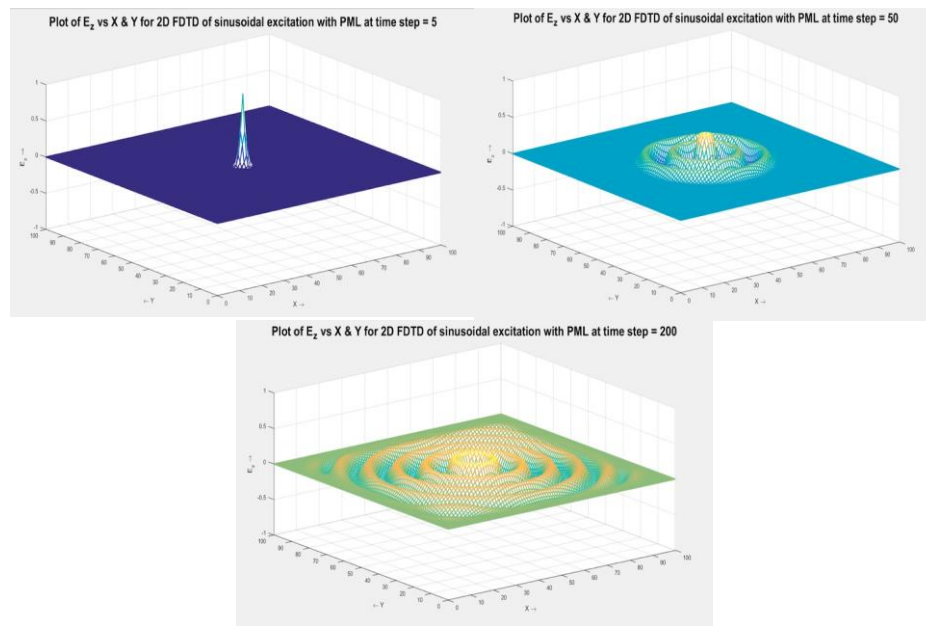


Fig. 5. The electric field along z -direction versus x - y and $\epsilon = 1$. Frequency= 3×10^7 Hz and number of cells=100 at different time steps.

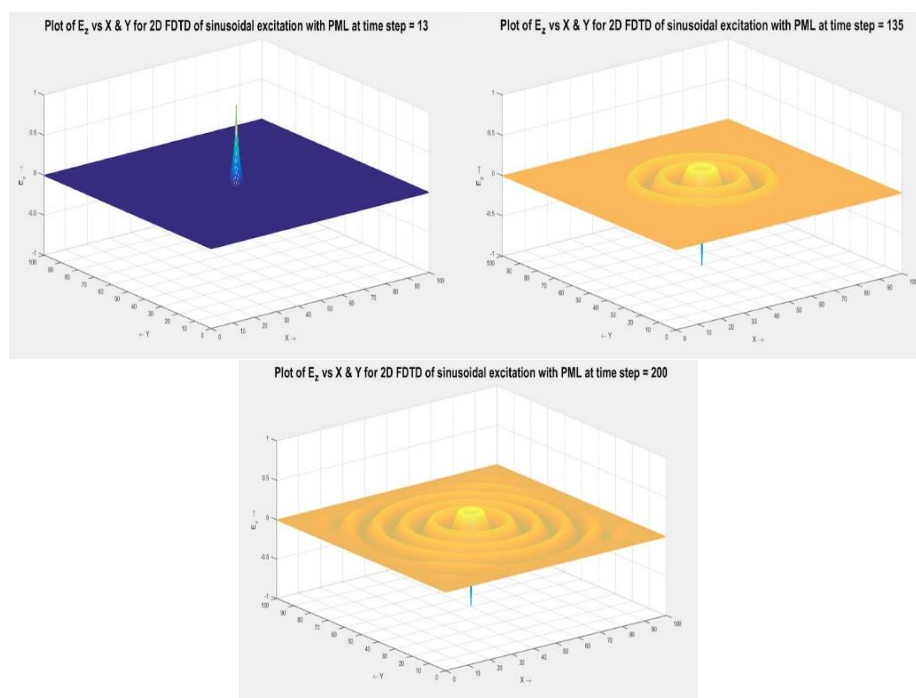


Fig. 6. The electric field along z -direction versus x - y and $\epsilon = 6$. Frequency= 3×10^7 Hz and number of cells=100 at different time steps.

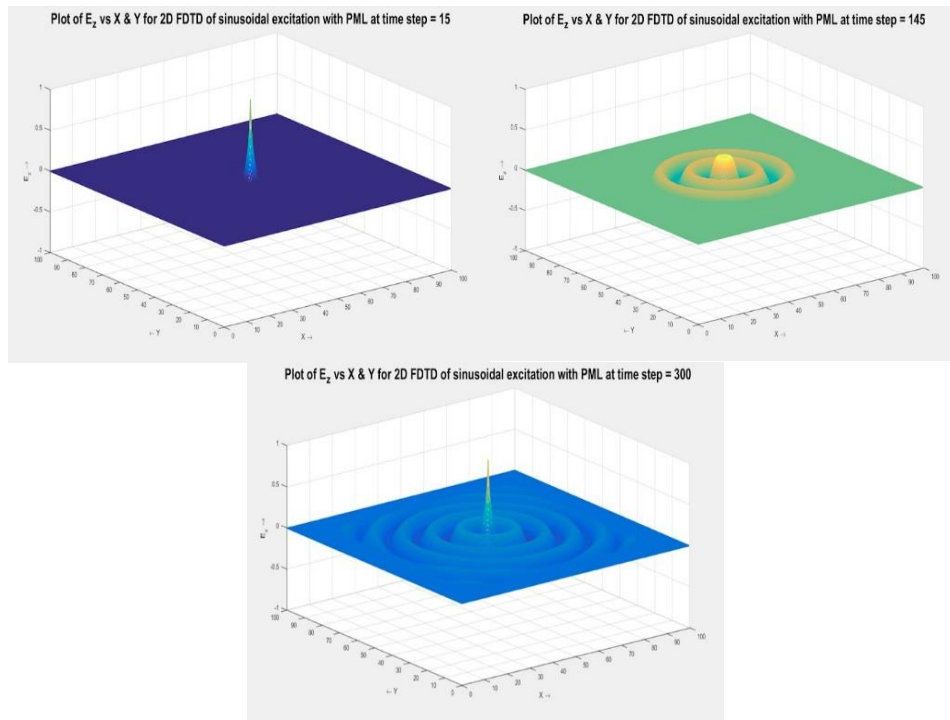


Fig. 7. The electric field along z-direction versus x-y and $\epsilon = 8$ Frequency= 3×10^7 Hz and number of cells=100 at different time steps.

It is well remarkable from figures (8-10) with the increase of the thickness up to 100, the wave propagation is changed in comparison with figures (5-7), even though keeping the same values of permittivity (by varying them from free space to dielectric medium). Here the time step is kept fixed for all cases.

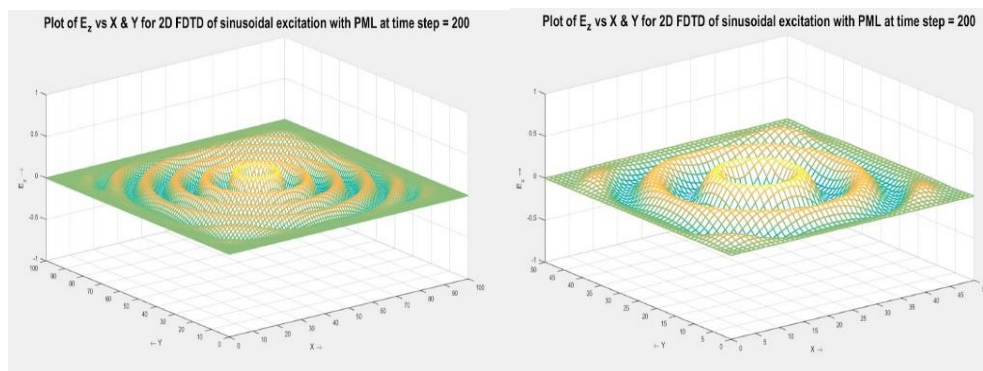


Fig. 8. The electric field along z-direction versus x-y and Frequency= 3×10^7 Hz for cell lattices=50 and 100 for left and right panel ($\epsilon = 1$).

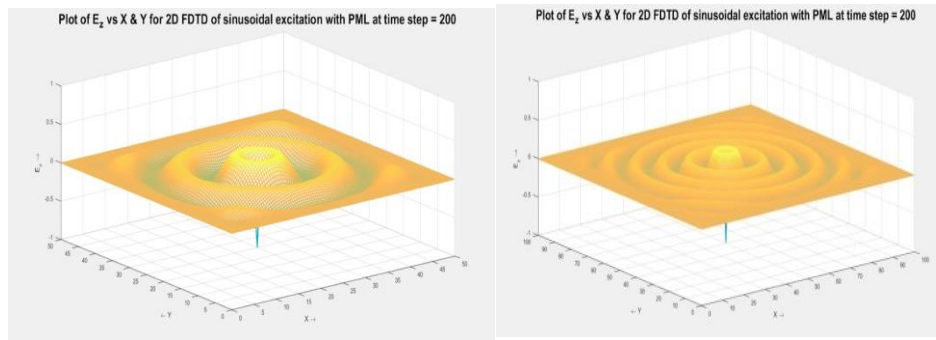


Fig. 9. The electric field along z -direction versus x - y and Frequency= 3×10^7 Hz for cell lattices=50 and 100 for left and right panel ($\epsilon=6$).

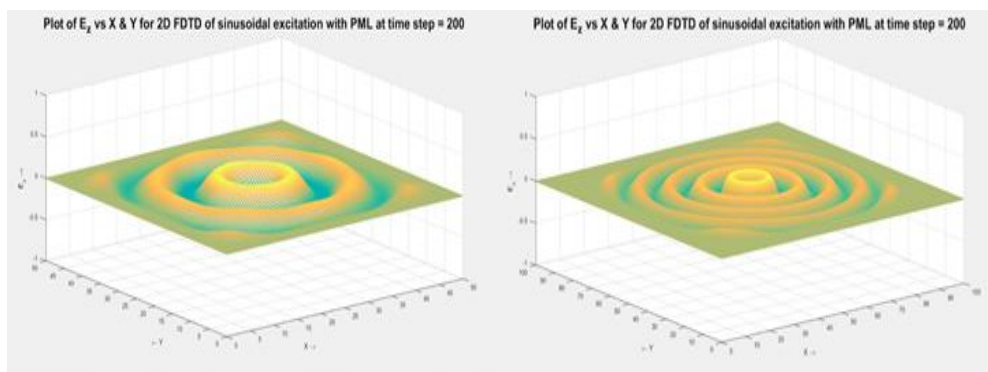


Fig. 10. The electric field along z -direction versus x - y and Frequency= 3×10^7 Hz for cell lattices=50 and 100 for left and right panel ($\epsilon=8$).

3.3. Wave guide in 2D systems

The structures are constructed in such way that a defective bended line is created. We simulated the electric field distribution E_z which is computed when varying the number of cells from 7 to 11 in x - y axis. As shown in Figs. (11-13), a thin dielectric slab composed of different cells along x - y direction shows that the light can also be confined in the horizontal direction and then it is dispersed in bended direction. This is due to the index contrast between the slab and its surrounding. Note that the source excitation is a Gaussian pulse with a carrier frequency of 5 GHz. Combined with the wave guiding along a line defect within the plane of the dielectric material, a possible 2D light confinement in dielectric materials can be established. Now, we keep the thin dielectric material with fixed cell=11 in x - y direction with variation of permittivity values from 5 to 11. It is well remarkable that the propagating wave displays a larger energy loss after certain time step for lower permittivity constant and the loss of energy is reduced with the increase of permittivity constant up to 11, as noticed in Figs. (14-16). The wave guiding in dielectric materials control the propagation characteristics for electric field distribution in these systems. However, it is clear from Figs. (17-19) that a total reflective light is occurring for negative permittivity values. This behavior is interesting in metallic wave guiding with negative permittivity media.

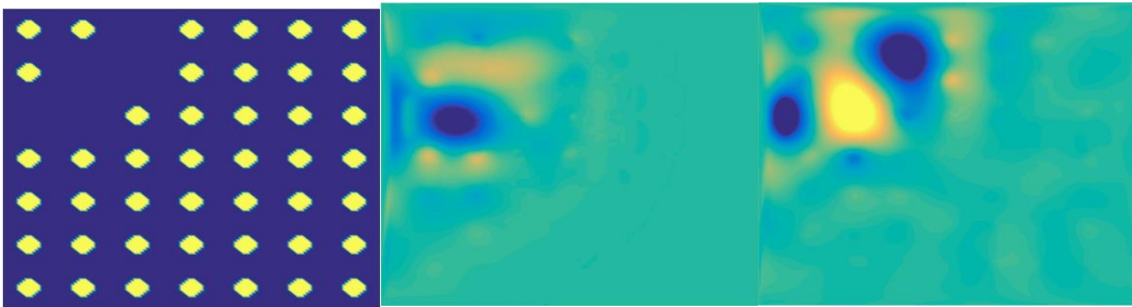


Fig. 11. The electric field distribution along z -direction versus x - y number of cells=7 and $\varepsilon = 11.4$.

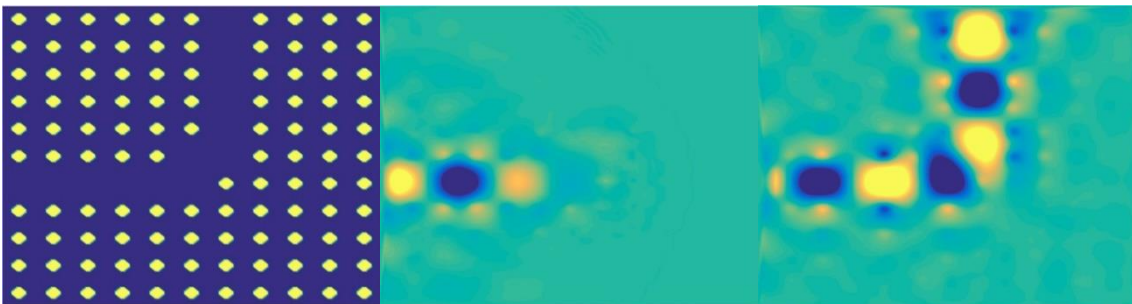


Fig. 12. The electric field distribution along z -direction versus x - y number of cells=11 and $\varepsilon = 11.4$.

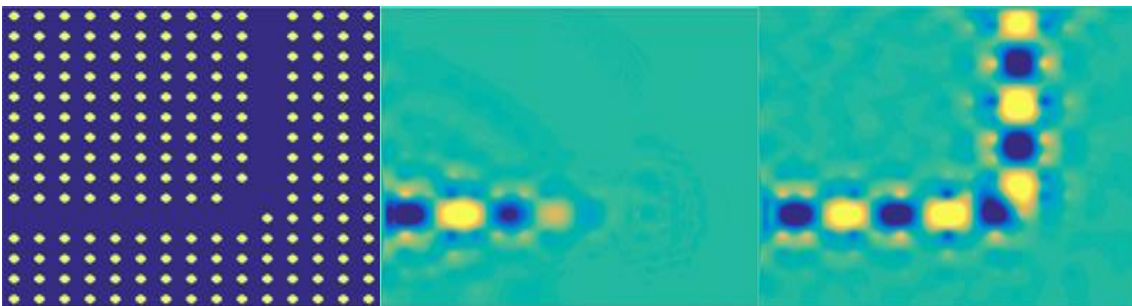


Fig. 13. The electric field distribution along z -direction versus x - y number of cells=15 and $\varepsilon = 11.4$.

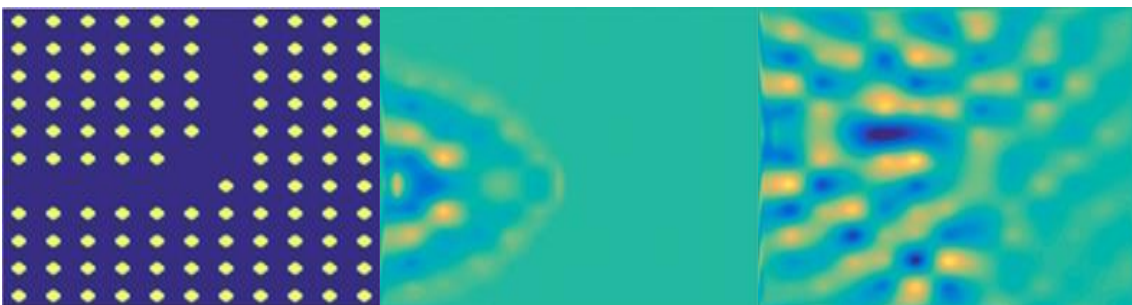


Fig. 14. The electric field along z -direction versus x - y for positive epsilon values ($\varepsilon=5$) and number of cells=11 at different time step.

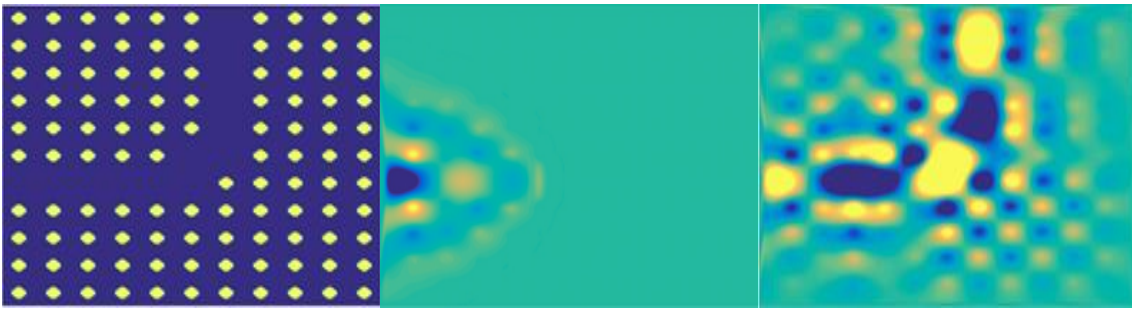


Fig. 15. The electric field along z-direction versus x-y for positive epsilon values ($\epsilon=7$) and number of cells=11 at different time step.

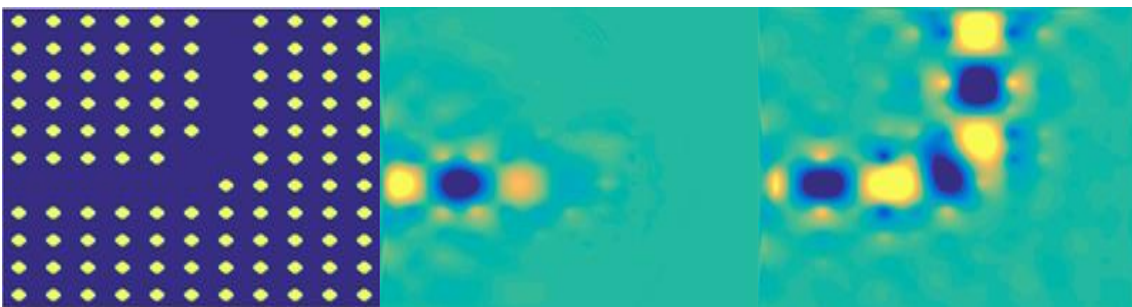


Fig. 16. The electric field along z-direction versus x-y for positive epsilon values ($\epsilon=11$) and number of cells=11 at different time step.

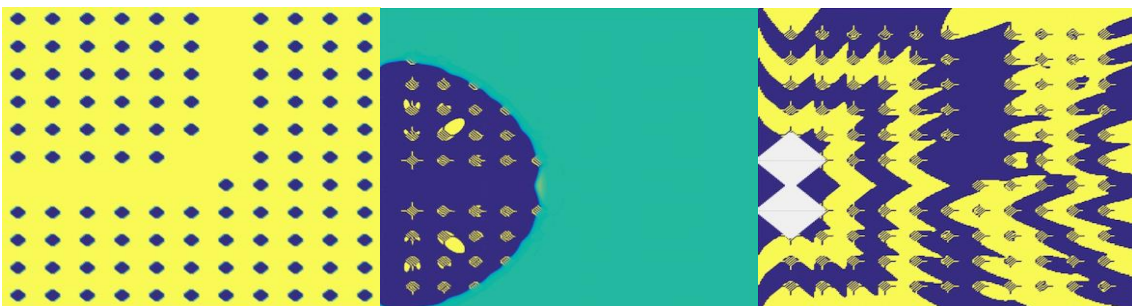


Fig. 17. The electric field along z-direction versus x-y for positive epsilon values ($\epsilon=-5$) and number of cells=11 at different time step.

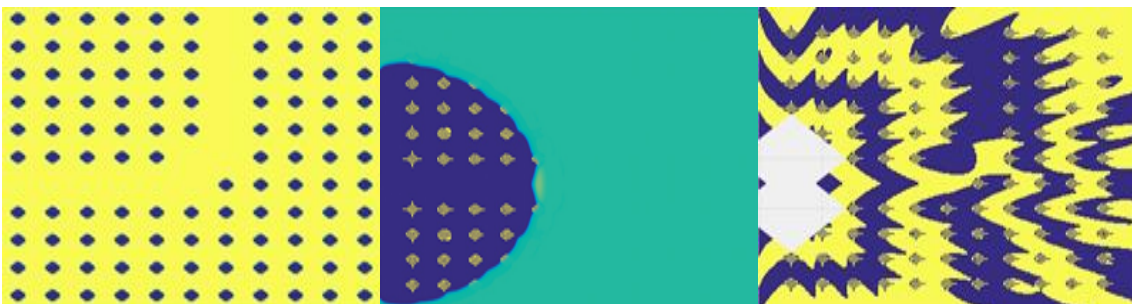


Fig. 18. The electric field along z-direction versus x-y for positive epsilon values ($\epsilon=-7$) and number of cells=11 at different time step.

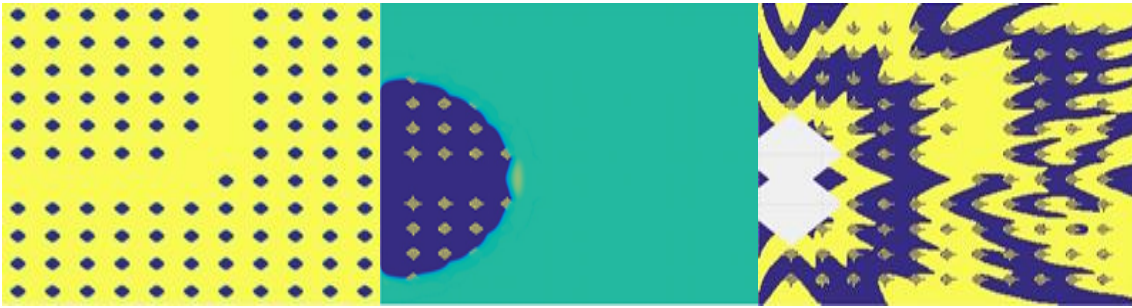


Fig. 19. The electric field along z -direction versus x - y for positive epsilon values ($\epsilon = -11$) and number of cell=11 at different time step.

3.4. The electric field distribution for dielectric materials and metamaterials

In one dimensional case, the electric field distribution varies with the variation of time step for the case of dispersive materials and metamaterials having positive and negative permittivity which is analyzed using FDTD method, as displayed in figure 20. The frequency of operation is given to be 0.7959 GHz for the purpose to provide a negative refractive index. The time step size is selected in such way to be much smaller than the mesh density. The related time step is computed by means of $\Delta(t) = 0.5, \Delta(x)/c$, and c represents the speed of light. The metamaterial cell is increased up to 100 cells. Outside this regime, the space is considered to be free space. The absorbing blocks are centered at center to truncate the problem space. A sinusoidal source was employed in the free- space regime. It is clear from Fig. 20 that the wave amplitudes in metamaterials are significant than the normal free space, as well as of dispersive region. It is hence the metamaterial increases the energy or intensity at the central regime. It is clear then the absorbing energy is maximum from the surrounding media.

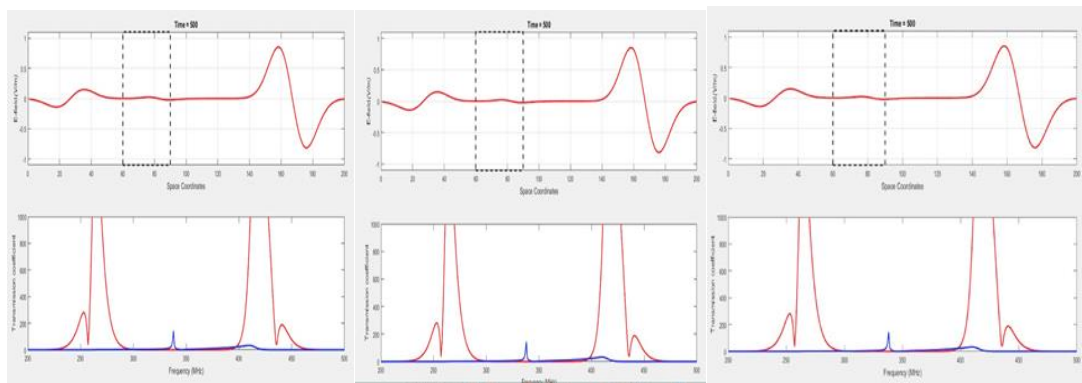


Fig. 20. Electric field distribution and transmission coefficient versus the frequency for positive epsilon values $\epsilon_2=2$, and $\epsilon_1=-2, 2$, and 6 for left, middle, and right panels.

3.5. Positive refractive index in dielectric material and negative refractive in metamaterials

The metamaterials are illustrating negative refractive index and own a characteristic not occurring in conventional materials. For this reason, metamaterials underscore notable capability for simplifying novel advancements in electromagnetism. In the case of one dimensional, the medium is considered; where the metamaterial slab is inserted between the two positive layers ($\epsilon > 0, \mu > 0$) layer. To formulate the metamaterial layer, the source frequency is equal to 0.7959 GHz

Our simulations are performed for negative-refractive index ($n=-2$) metamaterial in comparison with dielectric material having positive refractive index ($n=2$), as shown in figure 21.

The overall index of refraction refers to the medium in which the wave propagates through it. Here, the refraction at the interface of two media is considered positive for dielectric system and is negative for the case of metamaterial. Note that the transverse magnetic wave is set on x-y plane polarized magnetic field with components H_y and H_x and the polarization of the electric field E_z is set in a domain with two media with different permittivity constants. The space-step length is undertaken as 1 micron [18-19].

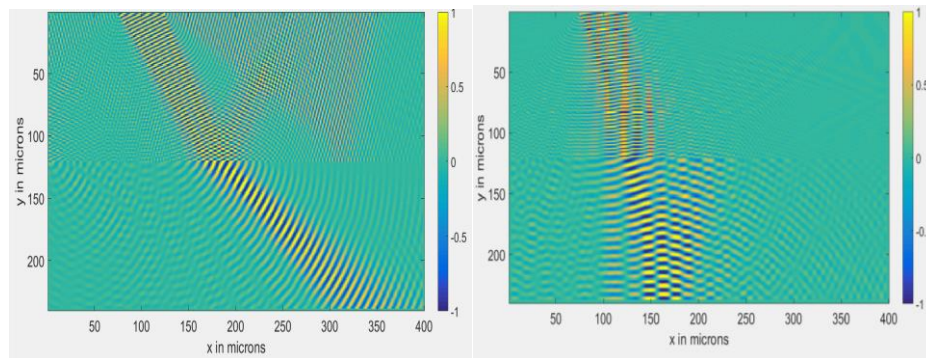


Fig. 21. Dielectric material with positive refractive index ($n=2$) for left and $n=-2$ for right.

4. Conclusion

The FDTD formulations is presented for modeling both dielectric and metamaterials by varying the dielectric constant of the medium and under the impact of layer thickness variation for 2D-materials.

-The increment in the number of cells shows a clear variation for the wave guiding both in dielectric and metamaterials systems.

-The metamaterial is able to enhance the amplitude of field component, irrespective with the normal dielectric media, when the wave is passing.

-In this case, the energy will be absorbed in metamaterial medium from the surrounding media.

-The source has also an important role in the absorption, transmission and reflection of electromagnetic wave. These systems would have potential applications, such as metamaterial superlens.

Acknowledgements

This research was funded by the Deanship of Scientific Research at Princess Nourah bint Abdulrahman University through the Fast-track Research Funding Program.

References

- [1] George V. Eleftheriades, Nader Engheta, Proceedings of the IEEE **99**, 10 (2011).
- [2] Nader Engheta, Richard W. Ziolkowski, Metamaterials: physics and engineering explorations, John Wiley and Sons, 2006.
- [3] T. Cui, D. Smith, R. Liu, Metamaterials Theory Design and Applications, Springer Berlin Heidelberg (2010).
- [4] I. A. Buriak et al., Journal of Nano-and Electronic Physics **8**(4), 4088 (2016).
- [5] A. N. Grigorenko, Optics letters **31**(16), 2483 (2006).
- [6] Natalie Wolchover, Physicists Close in on Perfect Optical Lens Based on Negative Refraction, Quanta Magazine, 2013, www.quantamagazine.org/physicists-close-in-on-perfect-optical-lens-

- based-on-negative-refraction-20130808/.
- [7] L. Billings, *Nature* **500**, 138 (2013).
 - [8] K. Inoue, K. Ohtaka, *Photonic Crystals Physics Fabrication and Applications*, Springer Berlin Heidelberg (2004).
 - [9] L. L. Lin, Z. Y. Li, K. M. Ho. *J. Appl. Phys* **94**, 811 (2003).
 - [10] J. Joannopoulos et al., *Photonics Crystal Modeling the Flow of Light*, 2ed Ed. Princeton University Press (2008).
 - [11] M. Maldovan, E. Thomas, *Periodic Materials and Interference Lithography for Photonics, Phononics and Mechanics*, Wiley-VCH Verlag GmbH & Co (2009).
 - [12] Guy Vandenbosch, *Computational Electromagnetics in Plasmonics, Plasmonics-Principles and Applications*. InTech, 2012.
 - [13] S. Rao, N. Balakrishnan, *Computational Electromagnetics a Review* (2013); Deshmukh R, Marathe D, Kulat KD. Design of Multiband Negative Permittivity Metamaterial Based on Interdigitated and Meander Line Resonator. In 2019 National Conference on Communications (NCC) 2019 Feb 20 (pp. 1-6). IEEE; Sougata Chatterjee (2020). METAMATERIAL 1D SIMULATION USING FDTD METHOD (<https://www.mathworks.com/matlabcentral/fileexchange/35530-metamaterial-1d-simulation-using-fdtd-method>), MATLAB Central File Exchange. Retrieved July 15, 2020; Soeren Schmidt (2020). Interactive Simulation Toolbox for Optics (<https://www.mathworks.com/matlabcentral/fileexchange/40093-interactive-simulation-toolbox-for-optics>), MATLAB Central File Exchange. Retrieved July 15, 2020.
 - [14] Dennis M. Sullivan, *Electromagnetic simulation using the FDTD method*. John Wiley and Sons, 2013.
 - [15] D. Markovich, K. Ladutenko, P. Belov, *Progress in Electromagnetics Research* **139**, 655 (2013).
 - [16] Sevgi, Levent, Gelişmiş Arama. Electromagnetic modeling and simulation, *Computational Electromagnetics (ICCEM)*, 2015 IEEE International Conference on, IEEE, 2015.
 - [17] Fumie Costen, Jean-Pierre Bérenger, Anthony K. Brown, *IEEE Transactions on Antennas and Propagation* **57**(7), 2014 (2009).
 - [18] V. ShadrivovIlya, Andrey A. Sukhorukov, Yuri S. Kivshar, *Physical Review E* **67**(5), 057602 (2003).
 - [19] George V. Eleftheriades, Nader Engheta, *Proceedings of the IEEE* **99**, 10 (2011).